Examination of the Nickel Site Structure and Reaction Mechanism in *Streptomyces seoulensis* Superoxide Dismutase

Suranjan B. Choudhury,[‡] Jin-Won Lee,[§] Gerard Davidson,[‡] Yang-In Yim,[§] Kurethara Bose,[‡] Manju L. Sharma,[‡] Sa-Ouk Kang,[§] Diane E. Cabelli,[||] and Michael J. Maroney*[,‡]

Department of Chemistry and the Program in Molecular and Cellular Biology, University of Massachusetts, Amherst, Massachusetts 01003-4510, Laboratory of Biophysics, Department of Microbiology, College of Natural Sciences and Research Center for Molecular Microbiology, Seoul National University, Seoul 151-742, Republic of Korea, and Department of Chemistry, Brookhaven National Laboratory, Upton, New York 11973

Received October 23, 1998; Revised Manuscript Received January 13, 1999

ABSTRACT: Superoxide dismutases are metalloenzymes involved in protecting cells from oxidative damage arising from superoxide radical or reactive oxygen species produced from superoxide. Examples of enzymes containing Cu, Mn, and Fe as the redox-active metal have been characterized. Recently, a SOD containing one Ni atom per subunit was reported. The amino acid sequence of the NiSOD deduced from the nucleotide sequence of the structural gene *sodN* from *Streptomyces seoulensis* is reported and has no homology with other SODs. X-ray absorption spectroscopic studies coupled with EPR of the Ni center show that the Ni in the oxidized (as isolated) enzyme is in a five-coordinate site composed of three S-donor ligands, one N-donor, and one other O- or N-donor. This unique coordination environment is modified by the loss of one N- (or O-) donor ligand in the dithionite-reduced enzyme. The NiSOD activity was determined by pulse radiolysis, and a value of $k_{cat} = 1.3 \times 10^9$ M^{-1} s^{-1} per Ni was obtained. The rate is pH sensitive and drops off rapidly above pH 8. The results characterize a novel class of metal center active in catalyzing the redox chemistry of superoxide and, when placed in context with other nickel enzymes, suggest that thiolate ligation is a prerequisite for redox-active nickel sites in metalloenzymes.

Superoxide dismutases (SOD, EC 1.15.1.1) are metalloenzymes that catalyze the disproportionation of superoxide to peroxide and molecular oxygen. As such, SODs are important components of systems that protect biological molecules from oxidative damage by superoxide or reactive oxygen species that can be generated from superoxide (*1*, *2*). Superoxide has been implicated as an agent in the aging process, inflammatory diseases, postischemic tissue injury, and a number of pathological conditions (*3*−*5*). Familial Amyotrophic Lateral Sclerosis is a neurodegenerative disease that has been linked to point mutations in CuZnSOD (*6*). The enzymes require the presence of a redox-active metal center, and examples of SODs containing Mn, Fe, or Cu (in a dinuclear site with Zn) are well-characterized (*1*, *2*, *7*−*10*). The redox-active metal centers in these enzymes are ligated by a combination of histidine imidazoles, aspartate carboxylates, and water, with the oxidized metal centers being five-coordinate. The dismutation reaction catalyzed by SODs proceeds via a mechanism wherein the metal is first reduced and then reoxidized by superoxide (eqs 1−3).

$$M^{(n+1)} + O_2^{\bullet -} \rightarrow M^{n+} + O_2 \quad (1)$$

$$M^{n+} + O_2^{\bullet -} + 2H^+ \rightarrow M^{(n+1)} + H_2O_2 \quad (2)$$

$$2O_2^{\bullet -} + 2H^+ \rightarrow O_2 + H_2O_2 \quad (3)$$

Recently, examples of SODs containing only Ni, NiSOD, have been isolated and characterized from various *Streptomyces* species (*11*−*13*). The amino acid composition, N-terminal amino acid sequences, and immunological properties show that NiSODs are distinct from the Mn, Fe, or CuZn enzymes, and thus represent a new class of SOD. We report here the results of X-ray spectroscopic studies of the Ni site structure in oxidized (resting) and dithionite-reduced NiSOD from *Streptomyces seoulensis*, and on the reaction mechanism in this NiSOD as examined by kinetic methods. These studies show that the coordination environment of NiSOD is unlike any previously characterized SOD, being composed largely of S-donor ligands. The analysis of kinetic data for the enzyme demonstrates that NiSOD is at least as active a catalyst for superoxide disproportionation as other known SODs. The spectroscopic and analytical data also suggest the possibility of a dinickel active site and implicate cysteinate ligands in the redox chemistry catalyzed by the enzyme.

EXPERIMENTAL PROCEDURES

Biochemistry. The samples of NiSOD used for XAS studies were obtained from *Streptomyces seoulensis* IMSNU

* Corresponding Author: Professor Michael J. Maroney, Department of Chemistry, Lederle Graduate Research Center Tower A, University of Massachusetts, Amherst, MA 01003-4510. Phone: 413-545-4876. Fax: 413-545-4490. E-mail: Mmaroney@chem.umass.edu.

[‡] University of Massachusetts.

[§] Seoul National University.

[||] Brookhaven National Laboratory.

10.1021/bi982537j CCC: $18.00
Published on Web 03/05/1999

21266^T as previously described (*13*) with minor modifications. Cells were grown under the previously described conditions except for the addition of 10 μM $NiCl_2$ to induce the NiSOD. Ammonium sulfate was added slowly up to 35% saturation to the crude extract prepared as previously described, and the precipitate was removed by centrifugation at 12000*g* for 30 min. The supernatant was loaded onto a Phenyl-Sepharose column (5 cm × 30 cm) equilibrated with 1.5 M ammonium sulfate in buffer A (50 mM sodium phosphate buffer, pH 7.4) and then eluted with a linear gradient of 0−1.5 M ammonium sulfate in buffer A. The active fractions were pooled and desalted with Sephadex G-25 column (8 cm × 60 cm) equilibrated with buffer A. The desalted fractions were purified by a Waters Delta Prep 4000 chromatography system with a Protein-Pak DEAE 5PW column (2.15 cm × 15 cm) and by preparative electrophoresis with a Bio-Rad Model 491 Prep Cell apparatus as described previously. After concentration of the active fraction with an Amicon YM10 membrane, these fractions were loaded onto a Superdex 200 column (HiLoad 16/60) equilibrated with buffer A and eluted with the same buffer by using a Pharmacia FPLC system. The active fractions were further purified on a Mono Q column (HR 5/5) with a linear gradient elution of 0−0.3 M NaCl on the same FPLC system. The active fractions of NiSOD were pooled and concentrated to 40 mg/mL with 30% glycerol in buffer A. The purity of the isolated enzyme was confirmed by SDS−PAGE.

The protein concentration of the oxidized sample was determined to be 1.83 mM (subunits) by amino acid analysis performed on an Applied Biosystems 420A/130A derivatizer-analyzer and 920A data module at the UMass Molecular and Cellular Biology Core Facility. The concentration of Ni in the sample was determined to be 1.82 mM by graphite furnace AA analysis performed at the UMass Environmental Analysis Laboratory of the Water Resources Research Center. The analytical results give a Ni/subunit ratio of 0.99. The sample of oxidized NiSOD used for spectroscopic studies was identical to that used for the protein and metal analyses. The sample of reduced NiSOD used for spectroscopic studies was prepared from an aliquot of the concentrated oxidized enzyme (50 μL) by the addition of a concentrated solution of dithionite (8.0 μL of a 0.6 M solution in buffer A). The final concentration of the reduced NiSOD sample was calculated to be 1.6 mM. For kinetic studies, the same oxidized sample was diluted to micromolar concentrations with distilled, deionized water.

Isolation of the S. seoulensis sodN Gene. The *S. seoulensis sodN* gene was identified from a recombinant EMBL3 (Stratagene) genomic library prepared with DNA isolated from *S. seoulensis* cultured in YEME medium (1% glucose, 0.5% bacto-peptone, 0.3% malt extract, 0.3% yeast extract, 10% sucrose, 5 mM $MgCl_2$) for 48 h at 30 °C. The library was constructed using the EMBL3/BamHI Vector Kit and propagated in *Escherichia coli* strain XL1-blue MRA(P2) (Stratagene). Recombinant plaques were transferred to nitrocelluose membranes and screened by hybridization with a 0.65 kb *Sma*I fragment from the *S. coelicolor sodN* gene (a gift from Dr. J.-H. Roe, Seoul National University) labeled with DIG as recommended by the supplier (Boehringer Manneheim). Further Southern hybridization analysis of phage DNA isolated from positive clones revealed a 0.7 kb *Apa*I-*Sal*I fragment that uniquely hybridized to the *S. coelicolor sodN* probe. The hybridization membranes were washed with 300 mM NaCl at room temperature for low stringency or with 15 mM NaCl at 68 °C for high stringency. The 0.7 kb *Apa*I-*Sal*I *S. soeulensis sodN* gene fragment was subcloned in pGEM-7Zf(+) (Promega) and designated pSODN1. Plasmid DNA was prepared using the Wizard Plus Minipreps DNA purification system (Promega) for ALF Express DNA sequencing (Pharmacia Biotech). The gene sequence reported here has been deposited in GenBank, accession number AF047461.

Spectroscopy. X-ray absorption spectroscopic (XAS) studies were carried out on the samples of oxidized (as isolated) and dithionite-reduced *Streptomyces seoulensis* (formerly *Streptomyces sp.* IMSNU-1) NiSOD described above. Two samples of the oxidized enzyme differing in sample batch and concentration were examined. The analyses of the data from both samples are in agreement regarding the structure of the Ni site, and only the data from the more concentrated sample is discussed further here.

XAS data were taken on beam line X9B at the National Synchroton Radiation Light Source (NSLS) at Brookhaven National Laboratory on samples held near 50 K in a cryostat under dedicated conditions at 2.58 GeV and 120−200 mA. A Si (220) double crystal monochromator internally calibrated to the first inflection point of Ni foil (8331.6 eV) was used. This arrangement provides a theoretical resolution of about 0.5 eV for the 0.5 mm hutch slit height employed. The spectra obtained using 0.2 eV steps had edge energies that were reproducible to within ±0.1 eV. Harmonic rejection was accomplished by using a focusing mirror left flat. X-ray fluorescence data were collected by using a 13-element Ge energy-discriminating fluorescence detector (Canberra). Maximum count rates were held at or below 30 kHz.

The integrity of the samples after ∼12 h of exposure to monochromatic synchrotron radiation was monitored in three ways: First, the energy of the Ni K-edge obtained from each sample was monitored on sequential scans. This allows changes in the sample (e.g., oxidation state) to be detected. No changes in either the oxidized or reduced enzyme were observed. Second, EPR spectra taken on each sample before and after exposure were compared and indicated no change in either sample. Third, the oxidized sample was assayed for activity before and after exposure by using the cytochrome *c* reduction method (*14*), and the exposed sample had 94% of the original activity.

The XAS data were analyzed according to previously published procedures (*15*). Correction of the background and normalization of the spectra as well as correction for detector efficiencies, absorbance by air and cryostat windows, and the variation with energy of the sample X-ray penetration depth were made by using standard procedures (*16*). For the purposes of comparison, the edge energy is taken to be the energy at a normalized absorbance of 0.5. The areas under the peaks assigned to 1s → 3d transitions were determined by fitting a background to the region of the spectrum immediately below and above this feature in energy and integrating the difference. Least-squares fits of the EXAFS data over a k range of 2.0−14 Å^{-1} were performed using Fourier-filtered data with a backtransform window of 1.1−2.6 Å (uncorrected for phase shifts) and single-scattering EXAFS theory (eqs I and II). Best fits were judged by

minimizing the goodness of fit criterion

$$\chi_c = \sum_{\text{shells}}\{NA[f(k)]k^{-1}r^{-2}e^{-2\sigma k^2}\sin(2kr + \alpha(k)\} \quad \text{(I)}$$

$$k = [4\pi m_e(E - (8340\text{ eV} + \Delta E))/h]^{1/2} \quad \text{(II)}$$

(GOF = $[n\{\text{idp}\}/(n\{\text{idp}\} - n\{\text{p}\})]^{1/2}R$, where R = ave[(data-simulation)/esd(data)], n(p) = the number of varied parameters, n(idp) = the number of data points for unfiltered refinements or $2(r_{max} - r_{min})(k_{max} - k_{min})/\pi$ for filtered refinements) and the difference in the disorder between model compounds and the fit ($|\Delta\sigma^2| = |(\sigma^2_{fit} - \sigma^2_{model})|$). Empirical parameters used in generating the EXAFS fits (amplitude reduction factors, A, Debye−Waller factors, σ, and values of E_0) were obtained from data on model compounds published elsewhere (*15*).

EPR spectra were obtained at X-band on a Bruker ESP 300 spectrometer. Spectra were recorded at 77 K on the samples used for XAS data collection by inserting polycarbonate XAS cuvettes into a liquid N_2 finger dewar.

Kinetics. Catalytic rate constants were measured by monitoring the disappearance of the O_2^- electronic absorbance at 260 nm, following generation of O_2^- by pulse radiolysis. All experiments were carried out in distilled water, which was passed through a Millipore ultrapurification apparatus. Sodium formate, monobasic potassium phosphate, sodium perchlorate, and ethylenediaminetetraacetic acid (EDTA) were of the highest purity commercially available. The pH of the solutions was adjusted by the addition of H_2SO_4 (double distilled from Vycor, GFS Chem. Co.) or NaOH (puratronic, Baker Chem. Co.). *Escherichia coli* MnSOD (Sigma Chemical Co.) and bovine CuZnSOD (DDI, Inc.) were used as purchased. The O_2 used was UHP grade (99.999%).

The pulse radiolysis experiments were carried out using the 2 MeV van de Graaff accelerator at Brookhaven National Laboratory. Dosimetry was established using the KSCN dosimeter, assuming a G value of 6.13 and a molar absorptivity of 7950 M^{-1} cm^{-1} at 472 nm for $(SCN)_2^-$. The path length was 2.0 cm. A 100−700 ns pulse width was used, resulting in the generation of 1−7 μM O_2^- per pulse. All experiments were carried out in 10 mM phosphate and 10 mM formate. Catalytic rate constants were obtained by following the disappearance of O_2^- at 260 nm in the presence of micromolar concentrations of NiSOD. The ionic strength studies were carried out at pH 7.0 in the presence of varying concentrations of $NaClO_4$. The reported rate constants for the NiSOD studies are based on metal concentration (not enzyme concentration), with the assumption that all of the metal is bound and active. This standardizes the rate constants between enzymes with different quaternary structure (NiSOD and MnSOD are tetramers while CuZnSOD is a dimer).

In addition to the determination of k_{cat} and its dependence on pH and ionic strength, the inhibition of the enzyme by NaN_3 was examined by measuring k_{cat} in the presence of 0.9−30 mM azide.

Upon radiolysis of water, the following radicals and molecules are generated:

$$H_2O \rightsquigarrow OH\ (2.75),\ e_{aq}^-\ (2.65),\ H\ (0.65),\ H_2\ (0.45),\ H_2O_2\ (0.70) \quad \text{(III)}$$

where the values in brackets are G values, that is, the number of atoms/molecules formed per 100 eV energy dissipated in the solution (*17*). Superoxide radicals were generated upon pulse radiolysis of an aqueous, air/O_2 saturated solution containing sodium formate according to the following mechanism:

$$OH + HCO_2^- \rightarrow H_2O + CO_2^- \quad (4)$$

$$CO_2^- + O_2 \rightarrow CO_2 + O_2^- \quad (5)$$

$$e_{aq}^- + O_2 \rightarrow O_2^- \quad (6)$$

$$H + O_2 \rightarrow HO_2 \quad (7)$$

where

$$HO_2 = O_2^- + H^+ \quad (8)$$

and pK_8 = 4.8 (*18*). Under our conditions, the formation of O_2^-/HO_2 radicals is more than 90% complete by the first microsecond after the pulse.

Kinetic data for NiSOD are compared with data obtained for bovine erythrocyte CuZnSOD and *E. coli* MnSOD. In all cases, the rate constants are given as a function of metal concentration and not enzyme concentration. The metal concentrations for NiSOD, CuZnSOD, and MnSOD were determined by atomic absorption measurements. In the case of CuZnSOD, it is important to eliminate any catalysis due to the presence of adventitious copper, since copper ions are more catalytically active than CuZnSOD. This was accomplished by the addition of EDTA to the assay medium. Measurements of catalytic activity carried out at pH 5 in the presence and absence of EDTA will effectively indicate any unbound copper, as CuEDTA is inactive. No such studies were carried out with either NiSOD or MnSOD since these metal ions are not catalytically active for superoxide dismutation to any appreciable extent relative to the enzymes. In these cases, it was assumed that all of the metal was bound and EDTA was not added to the assay solutions.

RESULTS

Primary Structure. The structural gene encoding NiSOD (*sodN*) was cloned and sequenced using standard procedures. Figure 1 shows the nucleotide sequence for *S. seoulensis sodN* and the deduced amino acid sequence arising from the nucleotide sequence and N-terminal analysis by Edman degradation. The nucleotide sequence has 90.84% homology with *Streptomyces coelicolor sodN* (*19*). An initiation codon (ATG) was found 42 bp (14 amino acids) upstream of the N-terminal His codon, suggesting that the NiSOD is processed through post-translational modification involving cleavage of this peptide, as is the case in *S. coelicolor* (*19*).

Ni Site Structure and Redox Chemistry. The reduction of NiSOD is accompanied by changes in the spectral properties of the Ni site that are consistent with the reduction of Ni(III) → Ni(II) and implicate this redox couple as the formal redox process involved in O_2^- disproportionation by NiSOD. The EPR spectra of the oxidized and reduced samples of Ni(SOD) used for XAS studies are shown in Figure 2. The spectrum shown was obtained from the oxidized NiSOD sample frozen at 77 K in a polycarbonate XAS holder before

```
1    5′ GTGACTCGGCGAGCCGAAGGTCGTAGCGCCCTGCC
     CCGCTCGGTCTCCTGCGACAGCTCCGGCATCCCCGGCACCTCCCCGGTCCGTTC
     CTCCACAGTCTCAGTGTGACCCCGGACTTTTGTCCTAAGCCCTGGGGGGCACTC
     GGGAAAACCAGTCCCTCAGGGAGTAATGTCCCACCTGAGAAGACGATCACGAGG
     AAGGAACGCTCCATGCTTTCCCGCCTGTTTGCCCCCAAGGTCAAGGTCAGCGCC
              M  L  S  R  L  F  A  P  K  V  K  V  S  A
     CACTGCGACCTGCCCTGCGGTGTGTACGACCCCGCCCAGGCCCGCATCGAGGCG
 1   H  C  D  L  P  C  G  V  Y  D  P  A  Q  A  R  I  E  A    18
     GAGTCGGTGAAGGCCATCCAGGAGAAGATGGCCGCCAACGACGACCTGCACTTC
19   E  S  V  K  A  I  Q  E  K  M  A  A  N  D  D  L  H  F    36
     CAGATCCGTGCCACGGTGATCAAGGAGCAGCGCGCCGAGCTGGCCAAGCACCAC
37   Q  I  R  A  T  V  I  K  E  Q  R  A  E  L  A  K  H  H    54
     CTGGACGTGCTCTGGAGCGACTACTTCAAGCCGCCGCACTTCGAGAGCTACCCC
55   L  D  V  L  W  S  D  Y  F  K  P  P  H  F  E  S  Y  P    72
     GAGCTGCACACCCTCGTCAACGAGGCTGTCAAGGCCCTCTCCGCCGCCAAGGCC
73   E  L  H  T  L  V  N  E  A  V  K  A  L  S  A  A  K  A    90
     TCCACGGACCCGGCGACGGGCCAGAAGGCCCTGGACTACATCGCCCAGATCGAC
91   S  T  D  P  A  T  G  Q  K  A  L  D  Y  I  A  Q  I  D   108
     AAGATCTTCTGGGAGACGAAGAAGGCTTGATCCTCCGGGTCACCCCTTCCGGCC
109  K  I  F  W  E  T  K  K  A  *
     TGCAACGTGTCTGATTTTGCAGTGTCCCCGAGGGCACCCGGCGCATTTGAGGCG
     CCGGGTGCG 3'   693
```

FIGURE 1: The DNA sequence of *sodN* and the deduced amino acid sequence of NiSOD from *Streptomyces seoulensis.* The putative ribosome binding site upstream of the open reading frame is underlined. The residues in bold face type indicate the 14 N-terminal amino acid determined by Edman degradation. The asterisk indicates the translational termination codon.

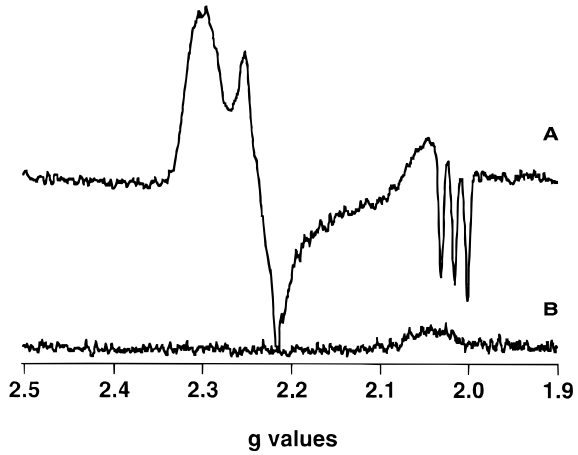

FIGURE 2: X-band EPR spectra taken at 77 K on the oxidized (A) and reduced (B) NiSOD samples used for XAS measurements.

data collection, is identical to previously published spectra of NiSODs, and shows an $S = 1/2$ signal ($g = 2.30$, 2.24, and 2.01) and hyperfine coupling ($A_{zz} = 24.9$ G) assigned to one axial N-donor ligand, features that are characteristic of a formally Ni(III) center in Ni(SOD) (*12*, *13*). Double integration of the EPR signals obtained from samples in EPR tubes over the temperature range of 100−250 K is consistent with 0.5 spins/Ni in the resting oxidized enzyme. With the exception of some line broadening, no significant changes in the EPR spectrum were observed at liquid He temperatures. The EPR signal characteristic of the oxidized enzyme is lost upon reduction with dithionite, consistent with the reduction of Ni(III) to Ni(II).

The region containing the X-ray absorption near edge structure (XANES) of the XAS spectra of the oxidized and reduced samples of NiSOD is shown in Figure 3. The apparent Ni K-edge energy of the samples is shifted from 8341.7(1) eV in the oxidized sample to 8340.5(1) eV in the reduced sample. The shift to lower values by 1.2 eV upon reduction indicates that the Ni center has more electron density in the reduced sample than in the oxidized sample.

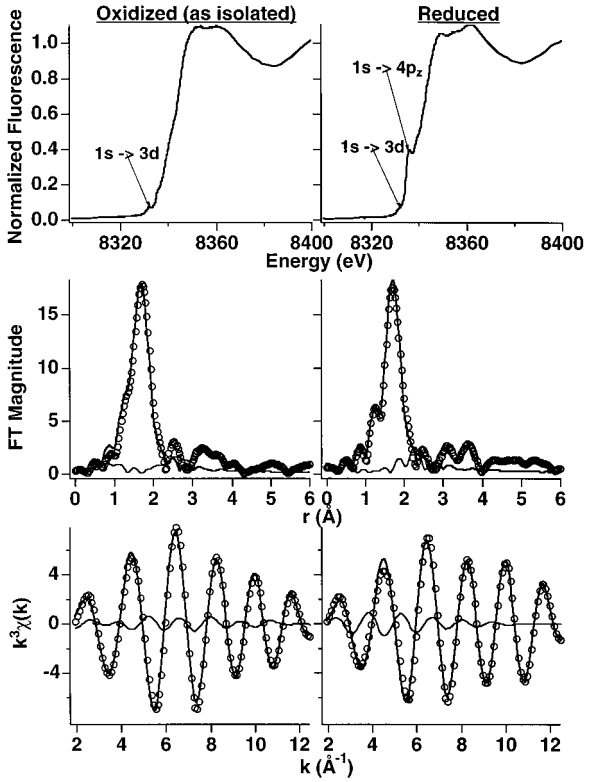

FIGURE 3: XAS spectra obtained for oxidized (left) and reduced (right) NiSOD: top, Ni K-edge XANES spectra; middle, Fourier transformed ($k = 2-14.0$ Å^{-1}) EXAFS data (circles), fits (bold solid lines), and differences (data fit, solid lines); bottom, Fourier-filtered (backtransform window = 1.1−2.6 Å, uncorrected for phase shifts) EXAFS data (circles), fits (bold solid line), and differences (solid line). The fit shown for oxidized NiSOD is OX4 in Table 1. The fit shown for reduced NiSOD is RE3 in Table 1.

The direction of this shift is consistent with the Ni(III) → Ni(II) formalism. However, the magnitude of the shift is smaller than the ∼2 eV shift expected for a one-electron redox process (*20*, *21*). Part of the reason for this small shift is that the shift in the Ni K-edge energy reflects a net increase

Table 1: Selected Curve-Fitting Results of Filtered EXAFS Spectra from NiSOD[a]

fit no.	shell	*N*	*r* (Å)	$\sigma^{2\,b}$ (x10^3 Å^2)	σ^2 (x10^3 Å^2)	correlations >0.6	GOF
			Oxidized				
OX1	1	4	Ni−S = 2.1522(9)	4.7(1)	1.5		0.51
OX2		6	Ni−N = 1.990(7)	2.9(8)	−1.5		2.48
OX3	2	1	Ni−N = 1.881(8)	5(1)	0.6		0.39
		4	Ni−S = 2.1552(8)	4.5(1)	1.3		
OX4		2	Ni−N = 1.909(4)	5.0(6)	0.6		0.36
		3	Ni−S = 2.1581(8)	2.9(1)	−0.3		
OX5		3	Ni−N = 1.927(4)	3.6(6)	−0.8		0.66
		2	Ni−S = 2.163(2)	0.8(2)	−2.4		
OX6	3	2	Ni−N = 1.91(1)	5(2)	0.6		0.35
		3	Ni−S = 2.158(3)	2.9(3)	−0.3		
		1	Ni−Ni = 2.88(6)	*17(8)*	11.5		
			Reduced				
RE1	1	4	Ni−S = 2.151(5)	4.3(5)	1.1		0.84
RE2		6	Ni−N = 1.99(3)	3(3)	−1.4		2.72
RE3	2	1	Ni−N = 1.87(2)	0(2)	−4.4		0.60
		3	Ni−S = 2.154(4)	2.1(4)	−1.1		
RE4		2	Ni−N = 1.91(1)	1(2)	−3.4	$\sigma_N^2/\sigma_S^2 = 0.68$	0.64
		2	Ni−S = 2.160(4)	0(4)	−3.2		
RE5		2	Ni−N = 1.86(4)	*10(6)*	5.6		0.71
		3	Ni−S = 2.155(4)	2.5(4)	−0.7		
RE6	3	1	Ni−N = 1.88(2)	0.0(2)	−4.4		0.57
		3	Ni−S = 2.154(3)	2.1(4)	−1.1		
		1	Ni−Ni = 2.88(5)	*12(7)*	6.5		

[a] $k = 2-14.0$ Å^{-1}; backtransform window = 1.1−2.6 Å (uncorrected for phase shifts). The distance (r) is for the absorber−scatterer pair indicated. Each unique absorber scattering interaction constitutes a shell. The root-mean-square disorder in r is σ^2; $\Delta\sigma^2$ are σ^2 relative to reference compounds. Correlations are indicated for all parameter cross-correlations with an absolute value of 0.6 or greater. GOF = $[n\{\text{idp}\}/(n\{\text{idp}\} - n\{\text{p}\})]^{1/2}R$, where R = ave[(data-simulation)/esd(data)], n(p) = the number of varied parameters, n(idp) = the number of data points for unfiltered refinements or $2(r_{max} - r_{min})(k_{max} - k_{min})/\pi$ for filtered refinements. [b] Underlined values are approaching physical insignificance. Large values of σ^2 suggest that the shell involved is badly disordered or has a coordination number that is too large and may be unnecessary for fitting the data.

in the electron density of Ni resulting from the combination of reduction and the loss of a ligand (vide infra). The loss of ligands is expected to moderate the change in charge density at the Ni arising from reduction alone.

The change in coordination number/geometry upon reduction of NiSOD is indicated by the analysis of XANES (Figure 3). The XANES data for the oxidized sample does not show a resolved maximum near 8338 eV that is associated with a $1s \rightarrow 4p_z$ electronic transition and is diagnostic for a planar coordination environment (*22*, *23*). The area under the peak associated with a $1s \rightarrow 3d$ electronic transition (0.046(5) eV) lies between values that are typical of five-coordinate (0.05−0.07 eV) and six-coordinate (0−0.04 eV) Ni sites (*22*). In contrast, the presence of a resolved peak near 8338 eV and a $1s \rightarrow 3d$ peak area of 0.047(5) eV demonstrates that that the Ni site in the reduced sample is planar, indicating a loss of one or two ligands upon reduction. The loss of axial ligands upon reduction of the Ni site is consistent with the known coordination chemistry of Ni(II) and Ni(III) complexes (*24*).

The analysis of the Ni K-edge EXAFS data for NiSOD shows that the ligand environment of the Ni center is unique among known SODs. Single-scattering analysis (*15*) of Fourier-filtered Ni K-edge EXAFS (Figure 3 and Table 1) over a k range of 2.0−14.0 Å^{-1} with a backtransform window of 1.1−2.6 Å (uncorrected for phase shifts) reveals that the data for both oxidized (as isolated) and dithionite-reduced *S. seoulensis* NiSOD are dominated by scattering from ∼3 S atoms at a distance of 2.16(2) Å. The best two shell fit to the data from the oxidized enzyme (Table 1, OX4) indicates a five-coordinate Ni environment composed of 2 N/O donors at a Ni−N/O distance of 1.909(4) Å and 3 S-donor ligands at distance of 2.158(1) Å. An alternative fit with four S-donors is ruled out by the amino acid content of the enzyme (vide infra), and a fit involving only 2 S-donors is a much poorer fit of the data. Upon reduction, the best two shell fit of the EXAFS data (Table 1, RE3) shows that the S-donor ligands become slightly shorter (3 Ni−S at 2.154(4) Å), while the number of N/O-donors and the Ni−N/O distance is decreased (1 Ni−N/O at 1.87(2) Å). The shorter bonds observed in the reduced protein are inconsistent with the redox chemistry and likely reflect the change in geometry from five- to four-coordinate.

Kinetic Studies. The activity of the NiSOD was determined using pulse radiolysis to generate superoxide and monitoring the rate of the disappearance of the superoxide electronic absorbance at 260 nm (*17*). The results indicate that the catalytic rate constant is 5.3×10^9 M^{-1} s^{-1} relative to the concentration of the tetrameric enzyme or 1.3×10^9 M^{-1} s^{-1} per Ni. No evidence for saturation was observed in these experiments. The catalytic rate constant measured for NiSOD is completely commensurate with the rate constant for CuZnSOD (≈1.2×10^9 M^{-1} s^{-1} per copper or 2.4×10^9 M^{-1} s^{-1} for the enzyme) under the same ionic strength conditions.

The catalytic rate constant is relatively pH-independent from pH 6−8 and then begins to decrease significantly. The data showing the dependence of k_{cat} as a function of pH are shown in Figure 4 in reference to the corresponding catalytic rate constants for bovine CuZnSOD and *E. coli* MnSOD under the same ionic strength and experimental conditions. The results confirm the pH dependence of NiSOD determined earlier over a wider pH range using an indirect assay (*13*), and show that the pH dependence is similar to those for other SODs, particularly MnSOD.

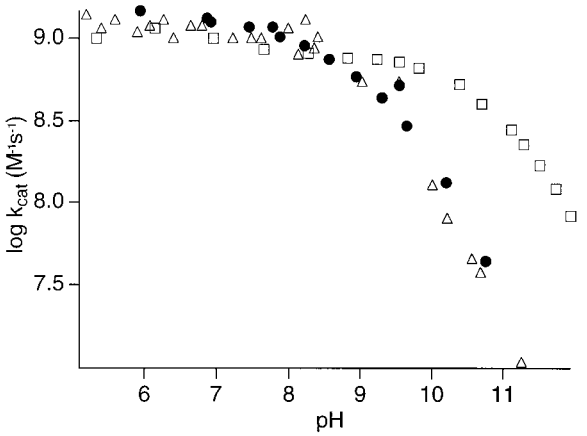

FIGURE 4: The dependence of k_{cat} on pH for NiSOD (solid circles), CuZnSOD (squares), and MnSOD (triangles).

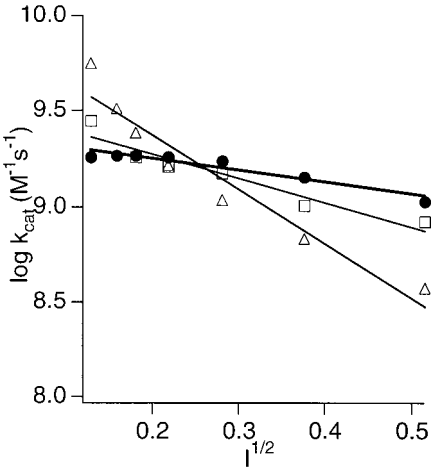

FIGURE 5: The dependence of k_{cat} on ionic strength for NiSOD (solid circles), CuZnSOD (squares), and MnSOD (triangles).

The NiSOD is only weakly inhibited by azide ion. The dependence of k_{cat} on the concentration of NaN_3 reveals that 42 mM azide is required for 50% inhibition. This result is consistent with previous measurements of the enzyme inhibition by indirect assay (*13*). The inhibition of NiSOD by azide ion is much weaker than for CuZnSOD, where the inhibition by N_3^- is competitive and has a $K_I = 12.7 \pm 1.1$ mM (*25*).

The catalytic rate constant of NiSOD was also measured as a function of ionic strength. Figure 5 shows a plot of the log of the observed rate constant versus the square root of the ionic strength for CuZnSOD, MnSOD, and NiSOD. As is apparent, MnSOD exhibits the strongest effect, while the effect on the NiSOD is the smallest. The ionic strength dependence of catalytic activity has been viewed as a measure of the electrostatic guidance of the anionic superoxide radical to the active site of the enzyme (*26*−*28*). In the case of CuZnSOD, the active site has a substantial positive charge, as reflected by the decrease in rate constant with increasing ionic strength. This decrease results from screening of the positive charge by the ions in solution. Studies employing a combination of site-directed mutagenesis, activity studies using pulse radiolysis, theoretical calculations, and NMR have been able to demonstrate the fine-tuning of the role of electrostatic attraction on the enzyme activity (*29*−*31*). This knowledge has been exploited with CuZnSOD to produce mutant enzymes with increased rate constants by changing residues near the active site channel from negatively charged residues to neutral residues (*31*). The same effect is observed upon chemical modification of amino acid residues in MnSOD. The ionic strength effect is seen most clearly by plotting the log of the calculated second-order rate constant (observed rate, s^{-1}, divided by the concentration of metal) as a function of the square root of the ionic strength of the solution. The latter term is the Debye−Huckel limit of the Bronsted−Bjerrum equation (log k(calc) = $(z^+z^-)I^{1/2} + C$; where z^+ and z^- are the charges of the ions). The fact that the NiSOD does not exhibit a large ionic strength dependence suggests that electrostatic guidance of superoxide ion is not an important aspect of the enzyme mechanism. It is worth noting that the similarity of the values of k_{cat} for all three enzymes in Figure 4 results from the arbitrary choice of an ionic strength where these rate constants are coincident (Figure 5).

During the studies of the ionic strength dependence and inhibition by azide, a decrease in k_{cat} from values recorded and obtained on previous runs was noted. This decrease in activity was traced to a slow inactivation of the enzyme over time at room temperature and in air. A sample intentionally left on the bench for 3 h lost ~50% of its activity. The origin of this decrease, which is not observed in either the MnSOD or CuZnSOD, is not known and could be due to a slow loss of metal from the enzyme under dilute conditions or to oxidative degradation.

DISCUSSION

S. seoulensis NiSOD is an α_4 tetramer composed of 13.4 kDa subunits (*13*). The primary structure of the NiSOD subunits provides additional information regarding the structure of the NiSOD active site. The sequence reveals that there are only two cysteine residues in the amino acid sequence of the mature enzyme. They occur near the N-terminus as a -cys-X-X-X-cys- motif, and both of these residues (cys_2 and cys_6) are implicated as ligands to the Ni center. However, three S-donor ligands are indicated by the EXAFS analysis of both oxidized and reduced NiSOD. The only other S-donor ligand in the mature enzyme is met_{28}. This leads to two plausible structures for the Ni site in NiSOD:

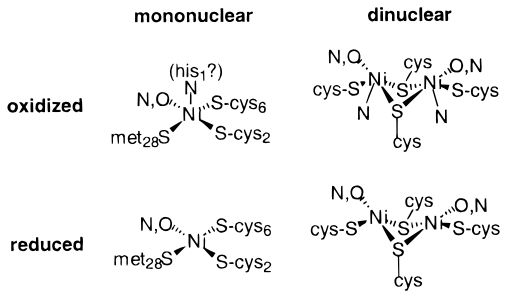

The presence of at least one axial N-donor ligand is indicated by the EPR spectrum of the oxidized enzyme. It is likely that it is this ligand that is lost upon reduction with dithionite. The identity of this N-donor ligand is not known, and there is little evidence in the Fourier transformed EXAFS spectra (Figure 2) to support the notion that it is a histidine ligand. However, the N-terminal residue, his_1, is a likely candidate for the axial N-donor because of its proximity to

the cys-X-X-X-cys sequence involved in ligation of the Ni center. If the Ni site is assumed to be mononuclear (one Ni per subunit), then the Ni *must* be coordinated by the single methionine residue in the mature protein (met_{28}) with a Ni−S distance similar to that of the cysS−Ni distances. Alternatively, ligation of the Ni by cysteinate residues alone requires a μ-dithiolato dinuclear active site composed of Ni atoms from two subunits, where one of the cysteine residues in each cys-X-X-X-cys sequence bridges the two Ni atoms. Such an arrangement is reminiscent of the Ni,Fe dinuclear site that has been characterized in *Desulfovibrio gigas* hydrogenase (*32*), where Ni is coordinated to four cysteinate ligands, two of which form bridges to the Fe atom.

A dinuclear Ni site in NiSOD is a possibility, considering the tetrameric quaternary structure of the holoenzyme and the N-terminal location of the two cysteine residues. A dinuclear site is also supported by the integration of the EPR signal in the oxidized enzyme (0.5 spins/Ni), and by the observation of EXAFS that can accommodate a second Ni atom at a distance of 2.88 Å in both the oxidized and reduced samples (Table 1, OX6 and RE6). Furthermore, the M−M distance obtained (2.88(6) Å) is similar to that observed in the hydrogenase crystal structure (2.9 Å) and in several μ-dithiolato nickel complexes (2.64−3.34 Å) (*22, 33*).

The redox chemistry of some μ-dithiolato nickel complexes is also consistent with the redox function of the NiSOD active site. The potentials involved in the oxidation and reduction of O_2^- at pH = 7 are −0.33 and 0.87 V, respectively. Thus, if these reactions are catalyzed by the alternate oxidation and reduction of a Ni site, this site must have a potential between these two values. The potentials of the Ni(II/III) and Ni(II/I) couples in aqueous media or with O/N-donor ligands lie outside this region at $\sim\pm$1.0 V (*34*−*36*). However, it is possible to drop the formal Ni(II/III) redox potential into this range using thiolate ligands (*37*), and several thiolate-bridged dinuclear complexes exhibit a single reversible, one-electron redox process near 0 V vs NHE. The oxidized complexes in these cases are associated with an $S = 1/2$ EPR signal that integrates to 0.5 spins/Ni (*21, 38*). Since the enzyme carries out one-electron redox chemistry, the ramification of a dinuclear structure for the active site of NiSOD is that only one redox equivalent is used per two metals. This situation is analogous to CuCuSOD (CuZnSOD where the Zn site is substituted by Cu) (*39*).

The cysteinate ligand environment found for NiSOD is unique among known SODs, but places NiSOD in line with the nickel sites found in other redox-active enzymes that contain nickel. These enzymes include carbon monoxide dehydrogenases (*40*), acetyl coenzyme synthase (*41*), methyl coenzyme M reductase (*42*), and [NiFe]hydrogenases (*32*), where thiolate ligation to the Ni center has been demonstrated either by crystallographic characterization or by EXAFS analysis. In contrast, the hydrolytic Ni enzyme urease (*43*) lacks thiolate ligation, as do the known Ni-binding proteins involved in Ni acquisition, transport, storage, and metallocenter assembly (*44, 45*). These results suggest that redox-active Ni centers in biology require thiolate ligation in order to operate at physiological redox potentials.

It is tempting to try to correlate these observations with potential reaction mechanisms for NiSOD. The mechanisms by which CuZnSOD, MnSOD, and FeSOD catalyze the disproportionation reaction of superoxide have been the subject of intense study (*1, 2*). The reduction and oxidation of the redox-active metal center occurs in two steps, either of which may occur by outer-sphere or inner-sphere electron transfer. It is documented that the oxidation of Mn(II)SOD occurs through the formation of an inner-sphere complex (*46*), while saturation is not observed except under the most extreme conditions with CuZnSOD (*25*). The fact that all of the oxidized enzymes bind small anions that act as inhibitors (e.g., N_3^- and CN^-) shows that it is possible for superoxide to access the active sites in these enzymes. Similarly, NiSOD is inhibited by CN^- but much less inhibited by N_3^- (*13*). In contrast, the reduced Fe(SOD) does not bind exogenous ligands, and the rates of ligand substitution in MnSOD and FeSOD are not fast enough to support the observed catalytic rates. Furthermore, there is evidence that azide binds to Arg in the reduced CuZnSOD (*47*), a residue that is responsible for 25% of the electrostatic steering of O_2^- in that enzyme. Thus it appears likely that reoxidation of the metal center occurs by an outer-sphere mechanism.

The use of S-donor ligands has an advantage in outer-sphere electron transport in that the more diffuse S orbitals can increase the efficiency of electron transport at greater distances, an effect that may account for the increased rates of superoxide dismutation that have been observed in hydrosulfide adducts of CuZnSOD (*48*). The smaller ionic strength effect observed for the NiSOD also suggests an outer-sphere mechanism. However, size and active site accessibility may also be factors. In addition to tuning the redox potential, the use of multiple thiolates further delocalizes the molecular orbital involved in the redox processes over several atomic centers.

The use of cysteinate ligands in a SOD active site is unanticipated, in part because metal thiolate complexes are sensitive to oxidation. Thus, outer-sphere reactions are particularly attractive for NiSOD in order to avoid the oxidation of thiolate ligands that is observed in Ni thiolate complexes in the presence of oxygen or peroxide, the products of superoxide dismutation (*49*−*51*). Oxidation of the NiSOD active site by superoxide might also be expected on the basis of the fact that one of the important biological targets damaged by superoxide are solvent-exposed Fe,S clusters such as that found in aconitase (*52*−*55*). This suggests that both redox reactions may occur by an outer-sphere mechanism in NiSOD, or that the thiolate ligands are well protected.

The observation of thiolate ligation in the NiSOD active site raises the possibility that the thiolate ligands might also serve as sites capable of donating protons that are essential in the reduction of superoxide to peroxide (*2*), as in eqs 9 and 10,

$$\mathrm{Ni(III)(^-SR)} + \mathrm{O_2^-} + \mathrm{H^+} \rightarrow \mathrm{Ni(II)(HSR)} + \mathrm{O_2} \quad (9)$$

$$\mathrm{Ni(II)(HSR)} + \mathrm{O_2^-} + \mathrm{H^+} \rightarrow \mathrm{Ni(III)(^-SR)} + \mathrm{H_2O_2} \quad (10)$$

which are Ni-specific versions of reactions 1 and 2. The role of metal thiols in proton transfer has been postulated in many enzymes including [NiFe]hydrogenases (*56*), and the formation of metal thiol complexes has been demonstrated in model compounds (*57*−*61*) including a dinuclear Ni complex (*62*). In the CuZnSOD, one of the protons required for the formation of H_2O_2 is believed to be obtained from the

reformation of the imidazolate bridge between the Cu and Zn ions upon oxidation of the reduced active site. The protonation and loss of this bridge upon reduction of the Cu site are important in order for the active site to retain the same positive charge in both the oxidized and reduced enzyme. The source of the other proton is unclear. In the case of MnSOD and FeSOD, these protons appear to be derived from a pool of protons involved in a hydrogen-bonding network that involves the water and Asp ligands and Tyr and Gln residues near the metal site.

ACKNOWLEDGMENT

Work performed at Seoul National University was supported by a research grant for the SRC (Research Center for Molecular Microbiology) from the Korea Science and Engineering Foundation (KOSEF). Work performed at the University of Massachusetts was supported by a grant from the NIH (GM38829, M.J.M.). The National Synchrotron Light Source, Brookhaven National Laboratory, is supported by the U.S. DOE, Div. of Materials Sciences and Div. of Chemical Sciences. Beamline X9B at NSLS is supported by NIH Grant RR-01633. Pulse radiolysis studies were carried out at Brookhaven National Laboratory under contract DE-AC02-98CH109916 with the U.S. Department of Energy and supported by its Division of Chemical Sciences, Office of Basic Energy Sciences.

REFERENCES

1. Miller, A. F., and Sorkin, D. (1997) *Comments Mol. Cell. Biophys. 9*, 1−48.
2. Cabelli, D. E., Riley, D., Rodriguez, J. A., Valentine, J. S., and Zhu, H. (1998) in *Biomimetic Oxidations Catalyzed by Transition Metal Complexes* (Meunier, B., Ed.) Chapter 10 (in press).
3. Halliwell, B. (1995) in *Active Oxygen in Biochemistry* (Valentine, J. S., Foote, C. S., Greenberg, A., and Liebman, J. F., Eds.) pp 313−335, Blackie Academic and Professional, New York.
4. Beyer, W., Imlay, J., and Fridovich, I. (1991) *Prog. Nucleic Acid Res. Mol. Biol. 40*, 221−253.
5. Wallace, D. C. (1992) *Science 256*, 628−632.
6. Brown, R. H. J. (1997) *Cold Spring Harbor Monogr. Ser. 34*, 569−586.
7. Tainer, J. A., Getzoff, E. D., Richardson, J. S., and Richardson, D. C. (1983) *Nature 306*, 284−287.
8. Tierney, D. L., Fee, J. A., Ludwig, M. L., and Penner-Hahn, J. E. (1995) *Biochemistry 34*, 1661−1668.
9. Lah, M. S., Dixon, M. M., Pattridge, K. A., Stallings, W. C., Fee, J. A., and Ludwig, M. L. (1995) *Biochemistry 34*, 1646−1660.
10. Borgstahl, G. E. O., Parge, H. E., Hickey, M. J., Beyer, W. F., Hallewell, R. A., and Tainer, J. A. (1992) *Cell*, 107−118.
11. Chun, J., Youn, H.-D., Yim, Y.-I., Lee, H., Kim, M. Y., Hah, Y. C., and Kang, S.-O. (1997) *Int. J. Syst. Bacteriol. 47*, 492−498.
12. Youn, H.-D., Youn, H., Lee, J.-W., Yim, Y.-I., Lee, J. K., Hah, Y. C., and Kang, S.-O. (1996) *Arch. Biochem. Biophys. 334*, 341−348.
13. Youn, H.-D., Kim, E.-J., Roe, J.-H., Hah, Y. C., and Kang, S.-O. (1996) *Biochem. J. 318*, 889−896.
14. Crapo, J. D., McCord, J. M., and Fridovich, I. (1978) *Methods Enzymol. 53*, 382−393.
15. Gu, Z., Dong, J., Allan, C. B., Choudhury, S. B., Franco, R., Moura, J. J. G., Moura, I., LeGall, J., Przybyla, A. E., Roseboom, W., Albracht, S. P. J., Axley, M. J., Scott, R. A., and Maroney, M. J. (1996) *J. Am. Chem. Soc. 118*, 11155−11165.
16. Scarrow, R. C., Maroney, M. J., Palmer, S. M., Que, L., Jr., Roe, A. L., Salowe, S. P., and Stubbe, J. (1987) *J. Am. Chem. Soc. 109*, 7857−7864.
17. Schwarz, H. A. (1981) *J. Chem. Educ. 58*, 101−105.
18. Bielski, B. H. J., Cabelli, D. E., Arudi, R. L., and Ross, A. B. (1985) *J. Phys. Chem. Ref. Data. 14*, 1041.
19. Kim, E.-J., Chung, H.-J., Suh, B., Hah, Y. C., and Roe, J.-H. (1998) *Mol. Microbiol. 27*, 187−195.
20. Kirby, J. A., Goodin, D. B., Wydrzynski, T., Robertson, A. S., and Klein, M. P. (1981) *J. Am. Chem. Soc. 103*, 5537−5542.
21. Maroney, M. J., Pressler, M. A., Mirza, S. A., Whitehead, J. P., Gurbiel, R. J., and Hoffman, B. M. (1995) *Adv. Chem. Ser. 246*, 21−60.
22. Colpas, G. J., Maroney, M. J., Bagyinka, C., Kumar, M., Willis, W. S., Suib, S. L., Mascharak, P. K., and Baidya, N. (1991) *Inorg. Chem. 30*, 920−928.
23. Eidsness, M. K., Sullivan, R. J., and Scott, R. A. (1988) in *The Bioinorganic Chemistry of Nickel* (Lancaster, J. R., Jr., Ed.) pp 73−91, VCH, New York.
24. Lappin, A. G., and McAuley, A. (1988) *Adv. Inorg. Chem. 32*, 241−294.
25. Fee, J. A., and Bull, C. (1986) *J. Biol. Chem. 261*, 13000−13005.
26. Cudd, A., and Fridovich, I. (1982) *J. Biol. Chem. 257*, 11443−11447.
27. Getzoff, E. D., Tainer, J. A., Weiner, P. K., Kollman, P. A., Richardson, J. S., and Richardson, D. C. (1983) *Nature 306*, 287−290.
28. Koppenol, W. H. (1981) in *Oxygen and Oxy-Radicals in Chemistry and Biology* (Rodgers, M. A., and Powers, E. L., Eds.) pp 671−674, Academic Press, New York.
29. Getzoff, E. D., Cabelli, D. E., Fisher, C. L., Parge, H. E., Viezzoli, M. S., Banci, L., and Hallewell, R. A. (1992) *Nature 358*, 347−351.
30. Fisher, C. L., Cabelli, D. E., Tainer, J. A., Hallewell, R. A., and Getzoff, E. D. (1994) *Proteins 19*, 24−34.
31. Banci, L., Bertini, I., Cabelli, D. E., Hallewell, R. A., Luchinat, C., and Viezzoli, M. S. (1991) *Free Radical Res. Commun. 12−13*, 239−251.
32. Volbeda, A., Garcin, E., Piras, C., de Lacey, A. L., Fernandez, V. M., Hatchikian, E. C., Frey, M., and Fontecilla-Camps, J. C. (1996) *J. Am. Chem. Soc. 118*, 12989−12996.
33. Choudhury, S. B., Pressler, M. A., Mirza, S. A., Day, R. O., and Maroney, M. J. (1994) *Inorg. Chem. 33*, 4831−4839.
34. Nag, K., and Chakravorty, A. (1980) *Coord. Chem. Rev. 33*, 87−147.
35. Haines, R. I., and McAuley, A. (1981) *Coord. Chem. Rev. 39*, 77−119.
36. Margerum, D. W., and Anliker, S. L. (1988) in *The Bioinorganic Chemistry of Nickel* (Lancaster, J. R., Jr., Ed.) pp 29−51, VCH, New York.
37. Fox, S., Wang, Y., Silver, A., and Millar, M. (1990) *J. Am. Chem. Soc. 112*, 3218−3220.
38. Kumar, M., Day, R. O., Colpas, G. J., and Maroney, M. J. (1989) *J. Am. Chem. Soc. 111*, 5974−5976.
39. Fielden, E. M., Roberts, P. B., Bray, R. C., Lowe, D. J., Mautner, G. N., Rotilio, G., and Calabrese, L. (1974) *Biochem. J. 139*, 49−60.
40. Tan, G. O., Ensign, S. A., Ciurli, S., Scott, M. J., Hedman, B., Holm, R. H., Ludden, P. W., Korszun, Z. R., Stephens, P. J., and Hodgson, K. O. (1992) *Proc. Natl. Acad. Sci. U.S.A. 89*, 4427−4431.
41. Xia, J., Dong, J., Wang, S., Scott, R. A., and Lindahl, P. A. (1995) *J. Am. Chem. Soc. 117*, 7065−7070.
42. Ermler, U., Grabarse, W., Shima, S., Goubeaud, M., and Thauer, R. K. (1997) *Science 278*, 1457−1462.
43. Gabri, E., Carr, M. B., Hausinger, R. P., and Karplus, P. A. (1995) *Science 268*, 998−1004.
44. Lee, M. H., Pankratz, H. S., Wang, S., Scott, R. A., Finnegan, M. G., Johnson, M. K., Ippolito, J. A., Christianson, D. W., and Hausinger, R. P. (1993) *Protein Sci. 2*, 1042−1052.

45. Allan, C. B., Wu, L.-F., Gu, Z., Choudhury, S. B., Al-Mjeni, F., Mandrand-Berthelot, M.-A., and Maroney, M. J. (1999) *Inorg. Chem. 38*, (in press).
46. Bull, C., Niederhoffer, E. C., Yoshida, T., and Fee, J. A. (1991) *J. Am. Chem. Soc. 113*, 4069−4076.
47. Leone, M., Cupane, A., Valeria, M., Stroppolo, M. E., and Desideri, A. (1998) *Biochemistry 37*, 4459−4464.
48. Searcy, D. G., Whitehead, J. P., and Maroney, M. J. (1995) *Arch. Biochem. Biophys. 318*, 251−263.
49. Mirza, S. A., Pressler, M. A., Kumar, M., Day, R. O., and Maroney, M. J. (1993) *Inorg. Chem. 32*, 977−987.
50. Mirza, S. A., Day, R. O., and Maroney, M. J. (1996) *Inorg. Chem. 35*, 1992−1995.
51. Grapperhaus, C. A., and Darensbourg, M. Y. (1998) *Acc. Chem. Res. 31*, 451−459.
52. Keyer, K., and Imlay, J. A. (1996) *Proc. Natl. Acad. Sci. U.S.A. 93*, 13635−13640.
53. Gardner, P. R., and Fridovich, I. (1991) *J. Biol. Chem. 266*, 19328−19333.
54. Flint, D. H., Tuminello, J. F., and Emptage, M. H. (1993) *J. Biol. Chem. 268*, 22369−22376.
55. Gardner, P. R., and Fridovich, I. (1991) *J. Biol. Chem. 266*, 1478−1483.
56. Dole, F., Fournel, A., Magro, V., Hatchikian, E. C., Bertrand, P., and Guigliarelli, B. (1997) *Biochemistry 36*, 7847−7854.
57. Sellmann, D., Becker, T., and Knoch, F. (1996) *Chem.−Eur. J. 2*, 1092−1098.
58. Sellmann, D., and Sutter, J. (1996) *ACS Symp. Ser. 653*, 101−116.
59. Sellmann, D., Mahr, G., Knoch, F., and Moll, M. (1994) *Inorg. Chim. Acta 224*, 45−59.
60. Stephan, D. W. (1984) *Inorg. Chem. 23*, 2207−2210.
61. Darensbourg, M. Y., Longridge, E. M., Payne, V., Reibenspies, J., Riordan, C. G., Springs, J. J., and Calabrese, J. C. (1990) *Inorg. Chem. 29*, 2721−2726.
62. Allan, C. B., Davidson, G., Choudhury, S. B., Gu, Z., Bose, K., and Maroney, M. J. (1998) *Inorg. Chem. 37*, 4166−4167.

BI982537J